

Hepatic NF- κ B-Inducing Kinase and Inhibitor of NF- κ B Kinase Subunit α Promote Liver Oxidative Stress, Ferroptosis, and Liver Injury

Xiao Zhong,^{1,2} Zhiguo Zhang ,¹ Hong Shen,¹ Yi Xiong,¹ Yatrik M. Shah,¹ Yong Liu,³ Xue-Gong Fan ,² and Liangyou Rui ^{1,4}

Drug-induced hepatotoxicity limits development of new effective medications. Drugs and numerous endogenous/exogenous agents are metabolized/detoxified by hepatocytes, during which reactive oxygen species (ROS) are generated as a by-product. ROS has broad adverse effects on liver function and integrity, including damaging hepatocyte proteins, lipids, and DNA and promoting liver inflammation and fibrosis. ROS in concert with iron overload drives ferroptosis. Hepatic nuclear factor kappa B (NF- κ B)-inducing kinase (NIK) is aberrantly activated in a broad spectrum of liver disease. NIK phosphorylates and activates inhibitor of NF- κ B kinase subunit alpha (IKK α), and the hepatic NIK/IKK α cascade suppresses liver regeneration. However, the NIK/IKK α pathway has not been explored in drug-induced liver injury. Here, we identify hepatic NIK as a previously unrecognized mediator for acetaminophen (APAP)-induced acute liver failure. APAP treatment increased both NIK transcription and NIK protein stability in primary hepatocytes as well as in liver in mice. Hepatocyte-specific overexpression of NIK augmented APAP-induced liver oxidative stress in mice and increased hepatocyte death and mortality in a ROS-dependent manner. Conversely, hepatocyte-specific ablation of NIK or IKK α mitigated APAP-elicited hepatotoxicity and mortality. NIK increased lipid peroxidation and cell death in APAP-stimulated primary hepatocytes. Pretreatment with antioxidants or ferroptosis inhibitors blocked NIK/APAP-induced hepatocyte death. **Conclusion:** We unravel a previously unrecognized NIK/IKK α /ROS/ferroptosis axis engaged in liver disease progression. (*Hepatology Communications* 2021;5:1704-1720).

Dietary nutrients (glucose, amino acids) and non-nutrient substances (drugs, xenobiotics) are absorbed from the gastrointestinal tract and transported to the liver. Hepatocytes not only metabolize/process nutrients to maintain metabolic homeostasis but also carry out detoxifications of drugs and xenobiotics to support life.^(1,2) As such, hepatocytes constantly experience metabolic stress,

oxidative stress, and/or other types of intracellular stress. Hepatocellular stress increases risk for hepatocyte injury/death, liver inflammation, and fibrosis.^(3,4) Liver oxidative stress is associated with liver disease, as illustrated by increased levels of reactive oxygen species (ROS) and reactive nitrogen species (RNS).⁽⁵⁻⁸⁾ ROS and RNS induce modifications on proteins, membrane phospholipids, and/or genomic

Abbreviations: 4-HNE, 4 hydroxynonenal; ALT, alanine aminotransferase; ANOVA, analysis of variance; APAP, acetaminophen; a.u., arbitrary units; β -gal, beta-galactosidase; BODIPY, boron-dipyromethene; CCL2, C-C motif chemokine ligand 2; CHX, cycloheximide; Con, control; CXCL5, C-X-C motif ligand 5; DAPI, 4',6-diamidino-2-phenylindole; DCF, 2',7'-dichlorofluorescein; FITC, fluorescein isothiocyanate; fl, flox; γ -H2AX, gamma-H2A histone family member X; GATA3, GATA binding protein 3; GSH, glutathione; h, hours; H&E, hematoxylin and eosin; Hep, hepatocyte; IKK α , inhibitor of nuclear factor kappa B kinase subunit alpha; IL, interleukin; iNOS, inducible nitric oxide synthase; JNK, c-Jun N-terminal kinase; MPO, myeloperoxidase; mRNA, messenger RNA; MTT, 3-(4,5-dimethylthiazol-2-yl)-2,5-diphenyltetrazolium bromide; NAC, N-acetyl-L-cysteine; NAPQI, N-acetyl-p-benzo-quinone imine; NF- κ B, nuclear factor kappa B; NIK, nuclear factor kappa B-inducing kinase; PBS, phosphate-buffered saline; qPCR, quantitative real-time reverse-transcription polymerase chain reaction; RNS, reactive nitrogen species; ROS, reactive oxygen species; TNF α , tumor necrosis factor alpha; TUNEL, terminal deoxynucleotidyl transferase-mediated deoxyuridine triphosphate nick-end labeling.

Received January 19, 2021; accepted May 11, 2021.

Additional Supporting Information may be found at onlinelibrary.wiley.com/doi/10.1002/hep4.1757/supinfo.

Supported by the National Institutes of Health (NIH) (grants RO1 DK114220, RO1 DK115646, and R21 AA025945 to L.R. and DK095201, CA148828, and CA245546 to Y.S.). This work used the cores supported by the Michigan Diabetes Research and Training Center (NIH DK020572), Michigan Metabolomics and Obesity Center (NIH DK089503), and the University of Michigan Gut Peptide Research Center (NIH DK34933).

DNA, leading to cellular dysfunctions, cell injury, and/or death.⁽⁸⁻¹⁰⁾ Oxidative stress-driven peroxidation of membrane phospholipids in concert with an iron overload underpins ferroptosis.^(11,12)

Nuclear factor kappa B (NF- κ B)-inducing kinase (NIK; also known as mitogen-activated protein kinase kinase kinase 14) is a serine/threonine kinase that mediates activation of the noncanonical NF- κ B2 pathway.⁽¹³⁾ NIK phosphorylates and activates inhibitor of κ B (I κ B) kinase- α (IKK α ; also referred to as Chuk), and IKK α in turn activates transcription factor NF- κ B2.⁽¹³⁻¹⁵⁾ NIK is activated by a wide range of stimuli, including a subset of cytokines, numerous endogenous metabolites and exogenous substances, and various cellular stress-inducing agents.^(13,15,16) Importantly, hepatic NIK is aberrantly activated in liver disease in mice and humans, including alcoholic liver injury, nonalcoholic fatty liver disease, hepatotoxin-induced liver injury, viral hepatitis, and autoimmune liver disease.⁽¹⁶⁻¹⁹⁾ We previously reported that a modest elevation of hepatic NIK in obesity augments hepatic glucose production, increasing the risk for type 2 diabetes.^(16,20) Consistently, hepatic NF- κ B2 also increases hepatic glucose production.⁽²¹⁾ Additionally, hepatic NIK promotes liver steatosis, presumably by suppressing peroxisome

proliferator-activated receptor alpha and fatty acid β oxidation.^(20,22) Aside from regulating metabolic pathways, hepatic NIK also blocks reparative hepatocyte proliferation, thereby impeding liver regeneration.⁽²³⁾ Furthermore, excessive activation of NIK causes hepatocytes to release mediators that potentially stimulate macrophages/Kupffer cells, leading to fatal immune destruction of the liver in mice.⁽¹⁹⁾

Acetaminophen (APAP) overdose is a leading cause for acute liver failure in Europe and North America.⁽²⁴⁾ APAP is a key constituent of Tylenol, which is commonly used to relieve fever and pain.⁽²⁾ APAP is converted to N-acetyl-p-benzo-quinone imine (NAPQI) by hepatocytes, and NAPQI increases hepatic oxidative stress and necrosis.^(2,25) APAP-induced ROS promotes calcium entry, worsening liver injury.⁽²⁶⁾ Considering that hepatocellular stress stimulates NIK, we speculated that APAP might activate hepatic NIK. NIK in turn promotes liver oxidative stress, mediating APAP hepatotoxicity. Given that ROS drives ferroptosis, we reasoned that hepatic NIK might augment hepatocyte ferroptosis in APAP-treated mice. We tested this hypothesis using both hepatocyte-specific NIK-knockout and NIK-overexpressing mice. Our results unveil a previously unrecognized NIK/IKK α /ROS/ferroptosis axis promoting liver disease progression.

© 2021 The Authors. *Hepatology Communications* published by Wiley Periodicals LLC on behalf of the American Association for the Study of Liver Diseases. This is an open access article under the terms of the Creative Commons Attribution-NonCommercial-NoDerivs License, which permits use and distribution in any medium, provided the original work is properly cited, the use is non-commercial and no modifications or adaptations are made.

View this article online at wileyonlinelibrary.com.

DOI 10.1002/hep4.1757

Potential conflict of interest: Nothing to report.

ARTICLE INFORMATION:

From the ¹Department of Molecular and Integrative Physiology, University of Michigan Medical School, Ann Arbor, MI, USA; ²Department of Infectious Diseases, Hunan Key Laboratory of Viral Hepatitis, Xiangya Hospital, Central South University, Changsha, China; ³College of Life Sciences, Institute for Advanced Studies, Wuhan University, Wuhan, China; ⁴Division of Gastroenterology and Hepatology, Department of Internal Medicine, University of Michigan Medical School, Ann Arbor, MI, USA.

ADDRESS CORRESPONDENCE AND REPRINT REQUESTS TO:

Liangyou Rui, Ph.D.
Department of Molecular and Integrative Physiology
University of Michigan Medical School
NCRC B20E 20-3825
2800 Plymouth Road
Ann Arbor, MI 48109, USA
E-mail: ruiy@umich.edu
Tel.: +1-734-615-7544

or
Xue-Gong Fan, M.D., Ph.D.
Department of Infectious Diseases
Hunan Key Laboratory of Viral Hepatitis
Xiangya Hospital, Central South University
87 Xiangya Road, Kaifu District, Changsha 410008, China
E-mail: xgfan@hotmail.com
Tel.: +86-731-8432-7392

Materials and Methods

ANIMALS

NIK^{lox (fl/fl)}, *IKK α ^{fl/fl}*, *Albumin-Cre*, hepatocyte (Hep)^{NIK}, and Hep^{Control (Con)} mice (C57BL/6J background) have been described.^(17,19,27) Mice were housed on a 12-hour light–dark cycle and fed *ad libitum* a normal chow diet (9% fat; TestDiet, St. Louis, MO).

ETHICS STATEMENTS

Animal research complied with relevant ethic regulations and was conducted following the protocols approved by the University of Michigan Institutional Animal Care and Use Committee.

APAP AND N-ACETYL-L-CYSTEINE TREATMENTS

Mice (8–10 weeks) were fasted overnight and injected intraperitoneally with a single dose of APAP (200–300 mg/kg body weight). Mice were pretreated with N-acetyl-L-cysteine (NAC; 300 mg/kg body weight, intraperitoneal) and then treated with APAP 5 minutes later. Blood samples were collected through tail veins. Plasma alanine aminotransferase (ALT) was measured using an ALT reagent set (Pointe Scientific Inc., Canton, MI). Livers were harvested 2–24 hours after APAP injection for biochemical and histologic analyses.

IMMUNOBLOTTING AND ROS ASSAYS

Liver tissue or hepatocyte cultures were homogenized in ice-cold lysis buffer (50 mM Tris HCl, pH 7.5, 0.5% Nonidet P-40, 150 mM NaCl, 2 mM ethylene glycol tetraacetic acid, 1 mM Na₃VO₄, 100 mM NaF, 10 mM Na₄P₂O₇, 1 mM phenylmethylsulfonyl fluoride, 10 μ g/mL aprotinin, 10 μ g/mL leupeptin). Tissue or cell extracts were resolved by sodium dodecyl sulfate–polyacrylamide gel electrophoresis and immunoblotted with the indicated antibodies (Supporting Table S1). Liver or cell extracts were incubated for 1 hour at 37°C with 5 μ M 2',7'-dichlorofluorescein (DCF), which is a diacetate fluorescent probe (D6883; Sigma). DCF levels were measured using a BioTek

Synergy 2 Multi-Mode Microplate Reader (485 nm excitation and 527 nm emission).

CELL CULTURE, ADENOVIRAL TRANSDUCTION, AND 3-(4,5-DIMETHYLTHIAZOL-2-YL)-2,5-DIPHENYLTETRAZOLIUM BROMIDE ASSAYS

Hepa1 and Huh7 hepatocytes were grown in Dulbecco's modified Eagle's medium supplemented with 5% fetal bovine serum (FBS), 100 units mL⁻¹ penicillin, and 100 μ g mL⁻¹ streptomycin. Primary hepatocytes were isolated from mice using type II collagenase (Worthington Biochem, Lakewood, NJ), as described.⁽²⁸⁾ Primary hepatocytes were grown on William's medium E (Sigma) supplemented with 2% FBS, 100 units mL⁻¹ penicillin, and 100 μ g mL⁻¹ streptomycin and transduced with β -galactosidase (β -gal) or NIK adenoviral vectors. After 12–14 hours of growth, hepatocytes were treated with APAP for 2–24 hours in the presence or absence of NAC, ferostatin-1 (Item No. 17729, CAS No. 347174-05-4; Cayman Chemicals), or liproxstatin-1 (Item No. 17730 CAS No. 950455-15-9, Cayman Chemicals). Hepatocyte viability was measured using colorimetric 3-(4,5-dimethylthiazol-2-yl)-2,5-diphenyltetrazolium bromide (MTT) assays (DOT Scientific Inc., Burton, MI).

IMMUNOSTAINING AND TERMINAL DEOXYNUCLEOTIDYL TRANSFERASE-MEDIATED DEOXYURIDINE TRIPHOSPHATE NICK-END LABELING ASSAYS

Liver frozen sections were prepared using a Leica cryostat (Leica Biosystems Nussloch GmbH, Nussloch, Germany), fixed in 4% paraformaldehyde for 30 minutes, blocked for 3 hours with 5% normal goat serum (Life Technologies) supplemented with 1% bovine serum albumin (BSA), and incubated overnight at 4°C with the indicated antibodies (Supporting Table S1). Liver sections were stained with terminal deoxynucleotidyl transferase-mediated deoxyuridine triphosphate nick-end labeling (TUNEL) reagents using an *in situ* cell death detection kit (#11684817910; Roche Diagnostics, Indianapolis, IN). Primary hepatocytes were grown

on glass coverslips, transduced with adenoviral vectors, treated with APAP, fixed in 4% paraformaldehyde, blocked with 5% normal goat serum, stained with TUNEL, DCF, or boron-dipyrromethene (BODIPY) 581/591 C11 probes, and visualized using a fluorescent microscope.

QUANTITATIVE REAL-TIME REVERSE-TRANSCRIPTION POLYMERASE CHAIN REACTION

Total RNA was extracted using TRIzol reagent (Invitrogen Life Technologies, Carlsbad, CA). First-strand complementary DNAs were synthesized using random primers and Moloney Murine leukemia virus (M-MLV) reverse transcriptase (Promega, Madison, WI). Quantitative real-time reverse-transcription polymerase chain reaction (qPCR) was performed using Radiant SYBR Green 2X Lo-ROX qPCR kits (Alkali Scientific, Pompano Beach, FL), a StepOnePlus Real-Time PCR System (Life Technologies Corporation, NY), and respective primers (Supporting Table S2).

FLOW CYTOMETRY

Mouse primary hepatocyte cultures were transduced with β -gal or NIK adenoviral vectors for 12 hours and followed by APAP stimulation (1 mM) for 24 hours. Hepatocytes were incubated with BODIPY 581/591 C11 (2.5 μ M) at 37°C for 30 minutes, trypsinized, centrifuged for 3 minutes at 200g, suspended in Hank's balanced salt solution containing 2% FBS, and applied to a Bio-Rad Ze5 cell analyzer. Hepatocytes were selected based on forward-scatter and side-scatter gating and were further analyzed following BODIPY 581/591 C11 staining through fluorescein isothiocyanate (FITC) gating. Data were analyzed using FlowJo software. Mean FITC-A was calculated on data from six independent experiments.

STATISTICAL ANALYSIS

Data were presented as means \pm SEM. Difference was analyzed by the two-tailed Student *t* test (two groups) and analysis of variance (ANOVA)/Bonferroni posttest (more than two groups) using GraphPad Prism 8. *P* < 0.05 was considered statistically significant. Survival rates were calculated using the Kaplan-Meier method.

Results

APAP TREATMENT UP-REGULATES HEPATIC NIK

To determine whether APAP treatment increases NIK expression and/or stability in the liver, we intraperitoneally injected C57BL/6J male mice with a single dose of APAP. APAP rapidly and substantially increased *NIK* messenger RNA (mRNA) levels in the liver (Fig. 1A). Increased NIK expression was detected within 2 hours after APAP injection (Supporting Fig. S1A). To determine whether APAP directly increases hepatocyte NIK expression, we stimulated Hepa1 cells (a murine hepatocyte line) with APAP. APAP robustly stimulated NIK expression in a time- and dose-dependent manner (Fig. 1B). To confirm these findings, we isolated primary hepatocytes from C57BL/6J mice and stimulated them with APAP. APAP increased NIK expression time/dose dependently in primary hepatocytes (Fig. 1C). Likewise, APAP treatment also increased NIK expression in Huh7 cells, a human hepatocyte line (Fig. 1D).

NIK is ubiquitously expressed, but its protein levels are low under baseline conditions due to rapid ubiquitination and degradation.^(13,16,19,29) To determine whether APAP increases NIK stability, we transduced mouse primary hepatocytes with NIK adenoviral vectors (*NIK* transcription is under the control of the constitutively active cytomegalovirus [CMV] promoter), followed by APAP stimulation. APAP substantially increased NIK protein levels (Fig. 1E). To directly assess NIK degradation, we transduced mouse primary hepatocytes with NIK adenoviral vectors and stimulated hepatocytes with APAP in the presence of the protein synthesis inhibitor cycloheximide (CHX). To avoid NIK overloading from APAP-treated cells, we loaded half the cell extracts from APAP-stimulated hepatocytes relative to phosphate-buffered saline (PBS)-treated hepatocytes (control). APAP stimulation considerably suppressed NIK degradation (Fig. 1F,G). To test if 26S proteasomes mediate NIK degradation, we treated primary hepatocytes with the proteasome inhibitor MG132 in conjunction with CHX. NIK degradation was detected at 4 hours but not 2 hours after CHX treatment (Fig. 1H, lanes 1, 2, and 4). MG132 treatment markedly inhibited NIK degradation (Fig. 1H, lane 4 vs. 5). Collectively, these

results demonstrate that APAP directly increases both expression and stability of NIK in hepatocytes.

To determine whether NIK up-regulation is a common signature of the hepatocyte response to hepatotoxins, we stimulated mouse primary hepatocytes with CCl₄. Chronic CCl₄ treatment is known

to increase liver *NIK* mRNA levels in mice.^(18,19) In accordance, CCl₄ directly stimulated expression of endogenous NIK in hepatocytes (Fig. 1I). To test if CCl₄ increases NIK stability, we transduced primary hepatocytes with NIK adenoviral vectors and stimulated them with CCl₄. CCl₄ dramatically increased

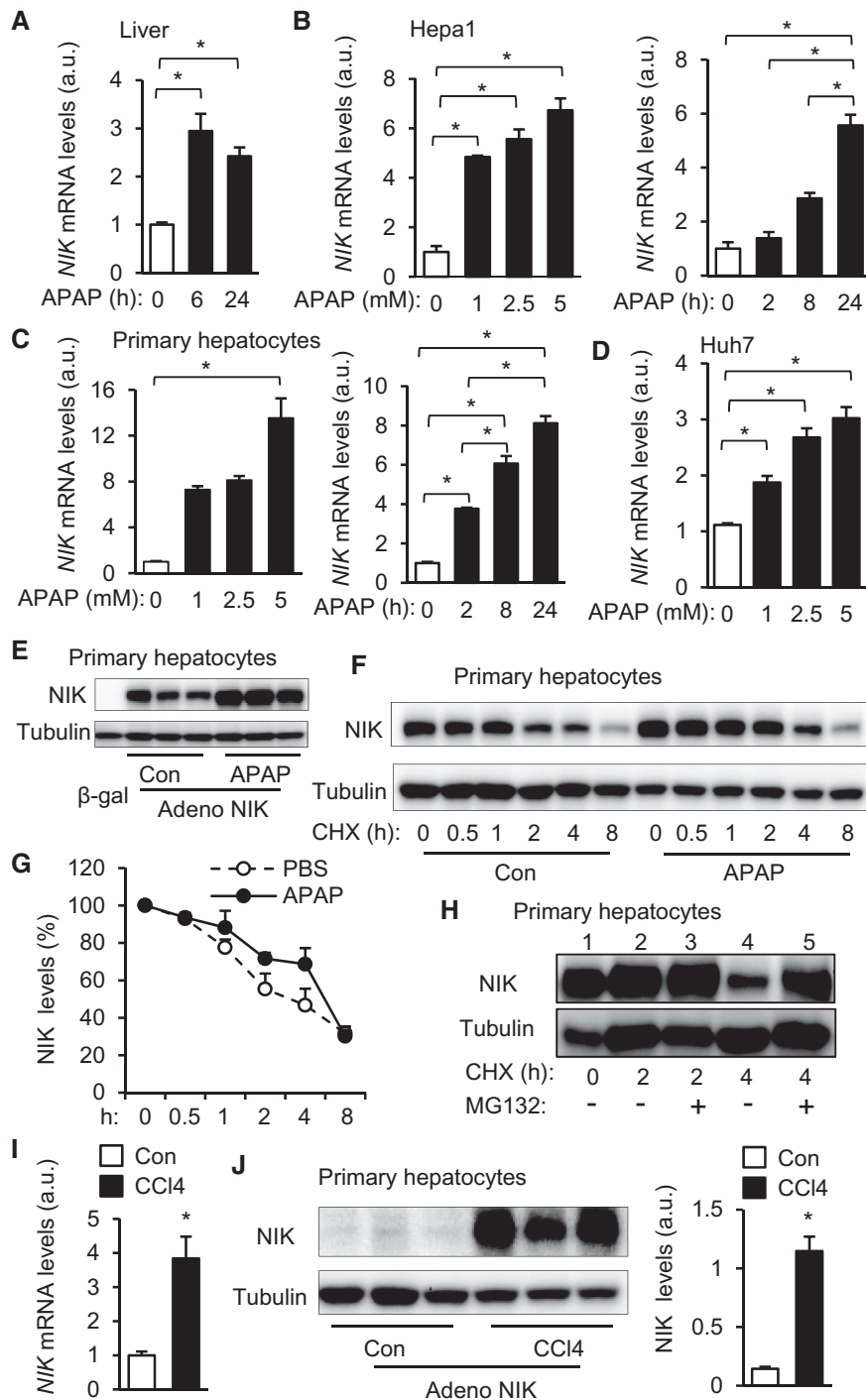


FIG. 1. APAP and CCl_4 treatments up-regulate hepatic NIK. (A) C57BL/6J male mice were treated with APAP (300 mg/kg body weight). Liver *NIK* mRNA levels were measured by qPCR and normalized to 36B4 expression ($n = 3-4$ per group). (B) *NIK* mRNA levels in APAP-treated Hepa1 cells (normalized to 36B4 expression, $n = 3$ per group). (C) *NIK* mRNA levels in mouse primary hepatocytes (normalized to 36B4 expression, $n = 3$ per group). (D) *NIK* mRNA levels in Huh7 hepatocytes (normalized to GAPDH expression, $n = 3$ per group). (E) Mouse primary hepatocytes were transduced with NIK or β -gal adenoviral vectors and treated with APAP or empty vehicles (Con) for 24 hours. Hepatocyte extracts were immunoblotted with antibodies to NIK and α -tubulin. (F,G) Mouse primary hepatocytes were transduced with NIK adenoviral vectors, pretreated with CHX, and followed by APAP stimulation. Hepatocyte extracts were immunoblotted with the indicated antibodies. NIK levels were normalized to α -tubulin levels and presented as percentage of initial values ($n = 4$ per group). (H) Mouse primary hepatocytes were transduced with NIK adenoviral vectors and treated with CHX and MG132. Hepatocyte extracts were immunoblotted with the indicated antibodies. (I) Mouse primary hepatocytes were stimulated with 2 mM CCl_4 for 24 hours. *NIK* mRNA levels were measured by qPCR (normalized to 36B4 levels, $n = 3$ per group). (J) Mouse primary hepatocytes were transduced with NIK adenoviral vectors and treated with 2 mM CCl_4 for 24 hours. Hepatocyte extracts were immunoblotted with the indicated antibodies. NIK levels were normalized to α -tubulin levels ($n = 3$ per group). Data are presented as mean \pm SEM. * $P < 0.05$; (A-D) one-way ANOVA/Bonferroni's multiple comparisons test; (G) two-way ANOVA/Bonferroni's multiple comparisons test; (I,J) two-tailed unpaired Student t test. Abbreviations: adeno, adenovirus; GAPDH, glyceraldehyde 3-phosphate dehydrogenase.

the levels of recombinant NIK (Fig. 1J). Thus, up-regulation of hepatic NIK (increased expression and stability) appears to be a common liver response to drugs, xenobiotics, and endogenous insults.

HEPATOCTYTE-SPECIFIC OVEREXPRESSION OF NIK AGGRAVATES APAP-INDUCED LIVER INJURY AND MORTALITY

To examine the role of NIK in acute liver failure, we generated hepatocyte-specific *NIK* transgenic mice (Hep^{NIK} ; genotype, *Rosa26-STOP-NIK^{+/-}; Cre^{+/-}*) by crossing *Rosa26-STOP-NIK* mice with *albumin-Cre* mice. *Rosa26-STOP-NIK* mice (referred to as Hep^{Con} hereafter) contain a *loxP-STOP-loxP-NIK* transgene knocked in the *Rosa26* locus, allowing Cre-dependent expression of recombinant NIK.⁽³⁰⁾ We previously verified that NIK is overexpressed specifically in the hepatocytes of Hep^{NIK} mice.⁽¹⁹⁾ Hep^{NIK} mice were grossly normal under baseline conditions. We intraperitoneally injected Hep^{NIK} and Hep^{Con} mice with a single dose of APAP. Strikingly, survival rates were substantially lower in Hep^{NIK} than in Hep^{Con} mice (Fig. 2A). Plasma ALT levels were dramatically higher in Hep^{NIK} than in Hep^{Con} mice (Fig. 2B). To validate liver failure, we examined liver histology. APAP injection caused liver necrosis as expected. Necrotic areas were significantly larger in Hep^{NIK} than in Hep^{Con} mice (Fig. 2C, hematoxylin and eosin [H&E] staining). Liver cell death was dramatically higher in Hep^{NIK} relative to Hep^{Con} mice (Fig. 2C, TUNEL staining). Liver neutrophil content was significantly higher in Hep^{NIK} relative

to Hep^{Con} mice, as assessed by staining liver sections with anti-myeloperoxidase (MPO) antibody (Fig. 2C). Liver expression of cytokines/chemokines (C-C motif chemokine ligand 2 [CCL2], C-X-C motif ligand 5 [CXCL5], interleukin (IL)-1 β , IL6, tumor necrosis factor α [TNF α]) was significantly higher in Hep^{NIK} relative to Hep^{Con} mice (Fig. 2D). Liver DNA damage was also higher in Hep^{NIK} than in Hep^{Con} mice, as assessed by staining liver sections with the antibody to gamma-H2A histone family member X (γ -H2AX; a DNA damage marker) (Fig. 2C).

To verify that NIK directly enhances APAP toxicity, we transduced primary liver cell cultures with NIK or β -gal adenoviral vectors, followed by APAP stimulation. APAP reduced hepatocyte viability (by MTT assays) in a time- and dose-dependent manner, as expected. Importantly, cell viability was significantly lower in NIK- than in β -gal-transduced hepatocytes (Fig. 2E). Taken together, these results unveil hepatic NIK as a previously unrecognized inducer for acute liver failure.

ABLATION OF HEPATIC NIK AMELIORATES APAP-INDUCED LIVER INJURY AND MORTALITY

To explore the role of endogenous hepatic NIK, we generated hepatocyte-specific *NIK* knockout (*NIK^{Δhep}*) mice (*NIK^{fl/fl}; Cre^{+/-}*) by crossing *NIK^{fl/fl}* mice with *albumin-Cre* drivers. *NIK^{fl/fl}* mice have been reported.⁽²⁰⁾ Considering that NIK deficiency might ameliorate liver injury, we increased APAP doses to 250 mg/kg body weight. Survival rates were substantially higher in

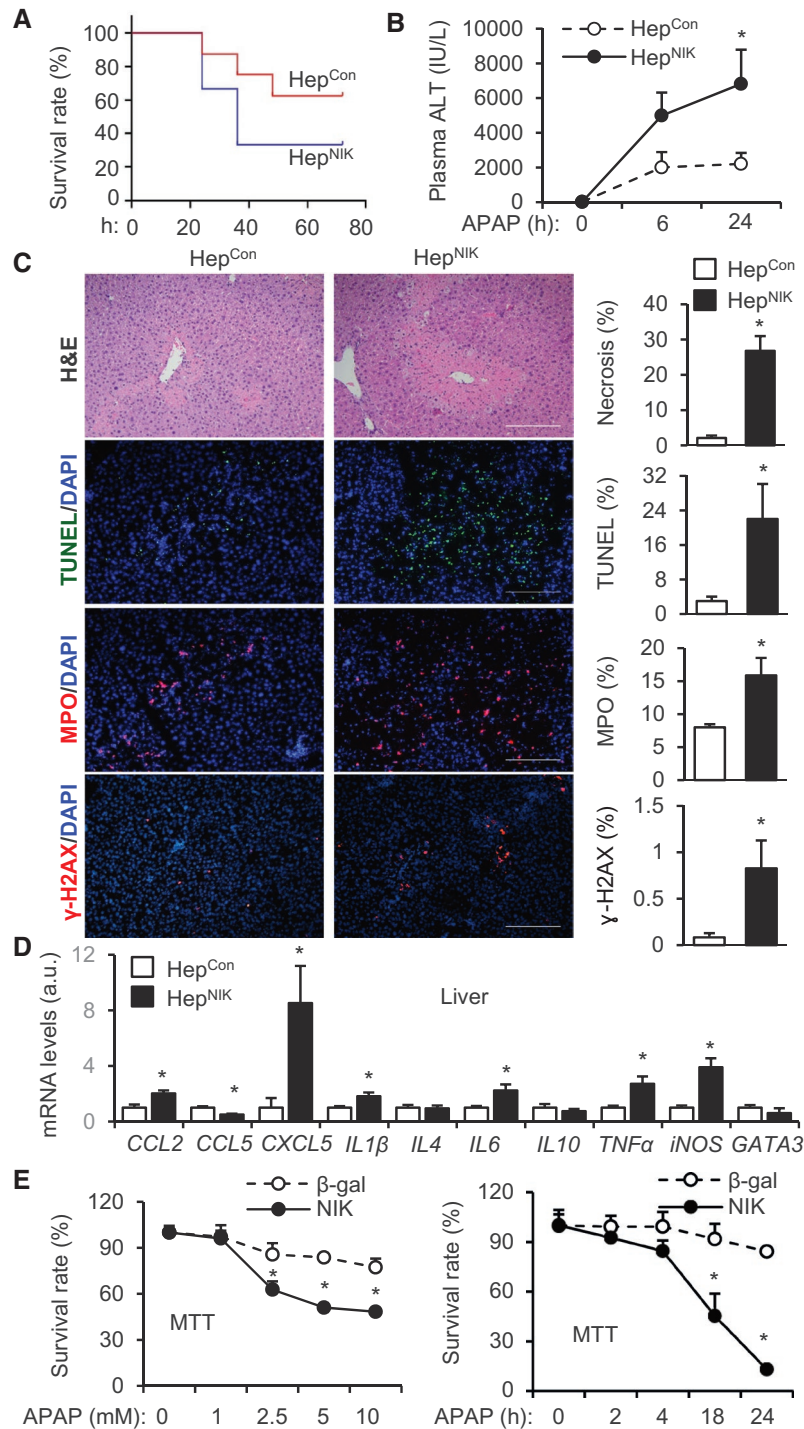


FIG. 2. Hep^{NIK} mice are prone to APAP-induced acute liver failure. (A) Survival rates following APAP treatment (300 mg/kg body weight). Male Hep^{NIK} mice, n = 6; male Hep^{Con} mice, n = 8. (B-D) Hep^{NIK} and Hep^{Con} male mice were treated with APAP (200 mg/kg). (B) Plasma ALT levels (n = 8 per group). (C) Liver sections were prepared 24 hours after APAP treatment and stained with the indicated agents. Necrotic area was normalized to total area. TUNEL, MPO, or γ-H2AX cell numbers were normalized to total cell number (n = 3-4 per group). Scale bar, 200 μm. (D) Liver gene expression 24 hours after APAP treatment (normalized to 36B4 levels, n = 4-8 per group). (E) Mouse primary hepatocytes were transduced with NIK or β-gal adenoviral vectors and treated with APAP. Hepatocyte viability was measured by MTT and normalized to baseline levels (n = 6 per group). Data are presented as mean ± SEM. *P < 0.05; (C,D) two-tailed unpaired Student *t* test; (B,E) two-way ANOVA/Bonferroni's multiple comparisons test.

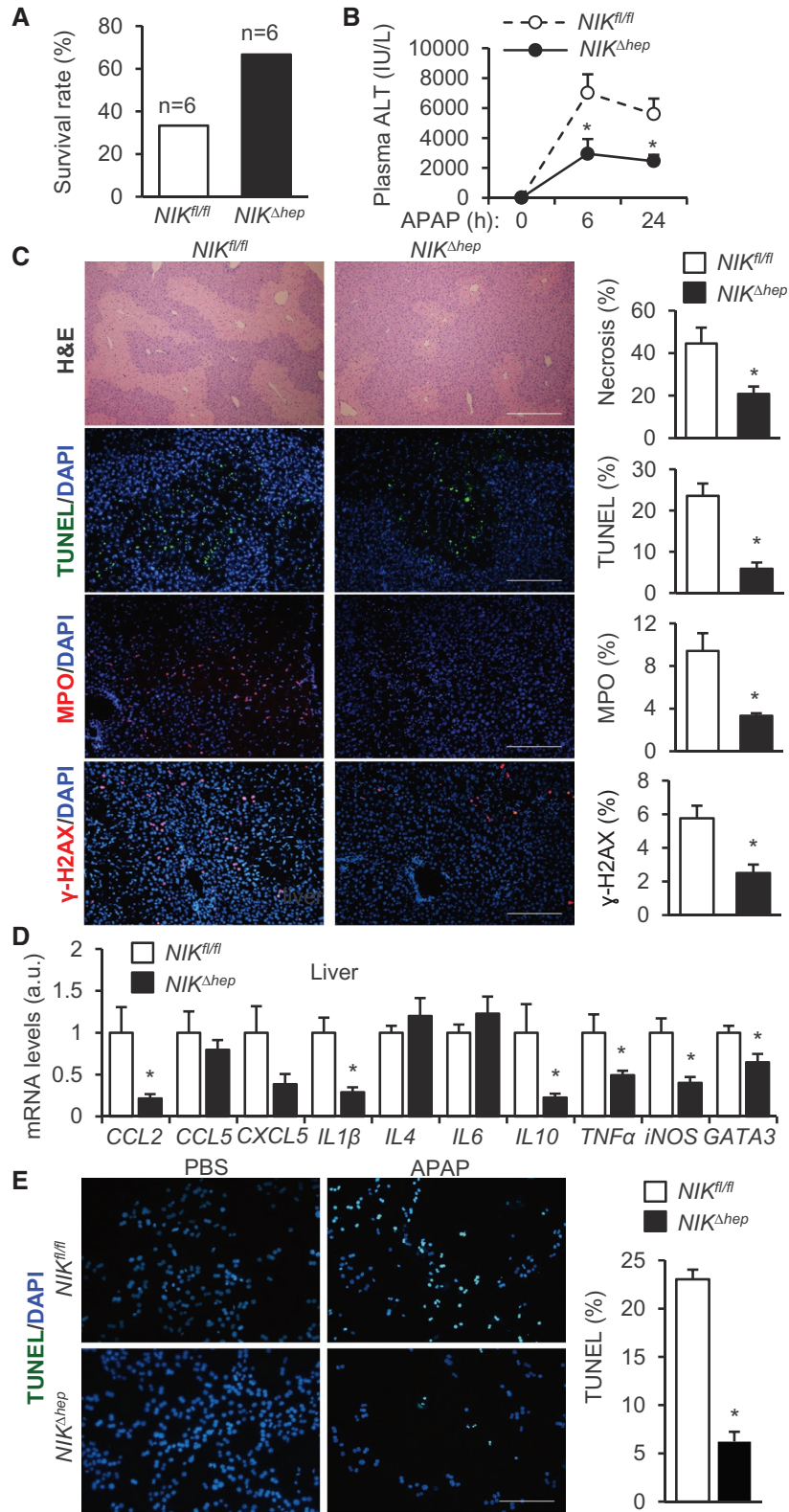


FIG. 3. *NIK*^{Δhep} mice are resistant to APAP-induced acute liver failure. (A-D) *NIK*^{Δhep} and *NIK*^{fl/fl} male mice were treated with APAP (250 mg/kg). (A) Survival rates 24 hours after APAP treatment (n = 6 per group). (B) Plasma ALT levels. *NIK*^{Δhep}, n = 15; *NIK*^{fl/fl}, n = 12. (C) Liver sections were stained with the indicated agents (24 hours after APAP treatment). Necrotic area was normalized to total area. TUNEL, MPO, or γ -H2AX cell numbers were normalized to total cell number (n = 4-12 per group). Scale bar, 200 μ m. (D) Liver gene expression 24 hours after APAP treatment (normalized to 36B4 levels, n = 9-12 per group). (E) Liver cells were prepared from *NIK*^{Δhep} and *NIK*^{fl/fl} mice, treated with APAP for 24 hours, and stained with TUNEL reagents. TUNEL⁺ cells were normalized to total cells (n = 3 per group). Data are presented as mean \pm SEM. **P* < 0.05; (C-E) two-tailed unpaired Student *t* test; (B) two-way ANOVA/Bonferroni's multiple comparisons test.

NIK^{Δhep} than in *NIK*^{fl/fl} mice after APAP treatments (Fig. 3A). Plasma ALT levels were significantly lower in *NIK*^{Δhep} than in *NIK*^{fl/fl} mice (Fig. 3B). Liver necrosis (H&E), hepatocyte death (TUNEL), liver DNA damage (γ -H2AX), and neutrophil infiltration into the liver (MPO) were all significantly lower in *NIK*^{Δhep} than in *NIK*^{fl/fl} mice (Fig. 3C). Liver expression of cytokines/chemokines (CCL2, IL1 β , IL10, TNF α) was lower in *NIK*^{Δhep} relative to *NIK*^{fl/fl} mice (Fig. 3D). *NIK*^{Δhep} female mice, like *NIK*^{Δhep} male mice, were also resistant to APAP-induced liver injury (Supporting Fig. S1B). To test if hepatic NIK influences APAP metabolism, we measured NAPQI production, as reported previously.⁽³¹⁾ We treated mice with APAP for 2 hours and immunoblotted liver extracts with antibodies recognizing NAPQI adducts. The levels of NAPQI protein adducts were comparable between *NIK*^{Δhep} and *NIK*^{fl/fl} mice (Supporting Fig. S2A). Likewise, liver NAPQI adduct levels were also comparable between APAP-treated Hep^{NIK} and Hep^{Con} mice (Supporting Fig. S2B). Thus, hepatic NIK appears to act downstream of or in parallel to NAPQI to augment APAP hepatotoxicity.

To further validate the role of NIK in APAP toxicity, we prepared primary liver cell cultures from *NIK*^{Δhep} and *NIK*^{fl/fl} littermates, stimulated cells with APAP, and measured cell death using TUNEL assays. APAP-induced liver cell death was significantly lower in the *NIK*^{Δhep} group relative to the *NIK*^{fl/fl} group (Fig. 3E). Together, these results demonstrate for the first time that endogenous hepatic NIK plays an important role in drug-induced liver injury.

ABLATION OF HEPATIC IKK α BLUNTS APAP-INDUCED LIVER INJURY

We next sought to identify downstream mediators coupling NIK to liver injury. We generated hepatocyte-specific *IKK α* -knockout (*IKK α* ^{Δhep}) mice by crossing

IKK α ^{fl/fl} mice with *albumin-Cre* mice. *IKK α* ^{fl/fl} mice have been described.⁽²⁷⁾ We treated *IKK α* ^{Δhep} and *IKK α* ^{fl/fl} littermates with APAP. Plasma ALT levels were significantly lower in *IKK α* ^{Δhep} than in *IKK α* ^{fl/fl} mice (Fig. 4A; Supporting Fig. S1C). Liver necrosis (H&E), hepatocyte death (TUNEL), liver DNA damage (γ -H2AX), and hepatic neutrophil infiltration (MPO) were substantially lower in *IKK α* ^{Δhep} relative to *IKK α* ^{fl/fl} mice (Fig. 4B). Expression of cytokines/chemokines in the liver (CCL2, CCL5, IL1 β) was significantly lower in *IKK α* ^{Δhep} mice (Fig. 4C). These results uncover the hepatic NIK/*IKK α* pathway as a previously unrecognized player in drug-induced liver injury.

NIK/IKK α PATHWAY MEDIATES APAP-INDUCED OXIDATIVE STRESS IN HEPATOCYTES

We next set out to investigate molecular mechanisms underlying NIK-promoted liver injury. We confirmed that APAP treatment robustly increased phosphorylation and activation of c-Jun N-terminal kinase (JNK)1/2 (Supporting Fig. S3). Liver JNK phosphorylation was slightly lower in *NIK*^{Δhep} relative to *NIK*^{fl/fl} mice (Supporting Fig. S3A) and was modestly higher in Hep^{NIK} than in Hep^{Con} mice 2 hours after APAP treatment (Supporting Fig. S3A). Twenty-four hours after APAP treatment, liver JNK phosphorylation was comparable both between *NIK*^{Δhep} and *NIK*^{fl/fl} mice and between Hep^{NIK} and Hep^{Con} mice (Supporting Fig. S3).

We reasoned that oxidative stress might couple the hepatic NIK/*IKK α* pathway to liver failure in APAP-treated mice. Indeed, liver ROS levels as measured by DCF probes were dramatically lower in APAP-treated *NIK*^{Δhep} (relative to *NIK*^{fl/fl}) and *IKK α* ^{Δhep} (relative to *IKK α* ^{fl/fl}) mice (Fig. 5A). Conversely, hepatic ROS was significantly higher in Hep^{NIK} than in Hep^{Con} mice 24 hours after APAP treatment (Fig. 5A). To

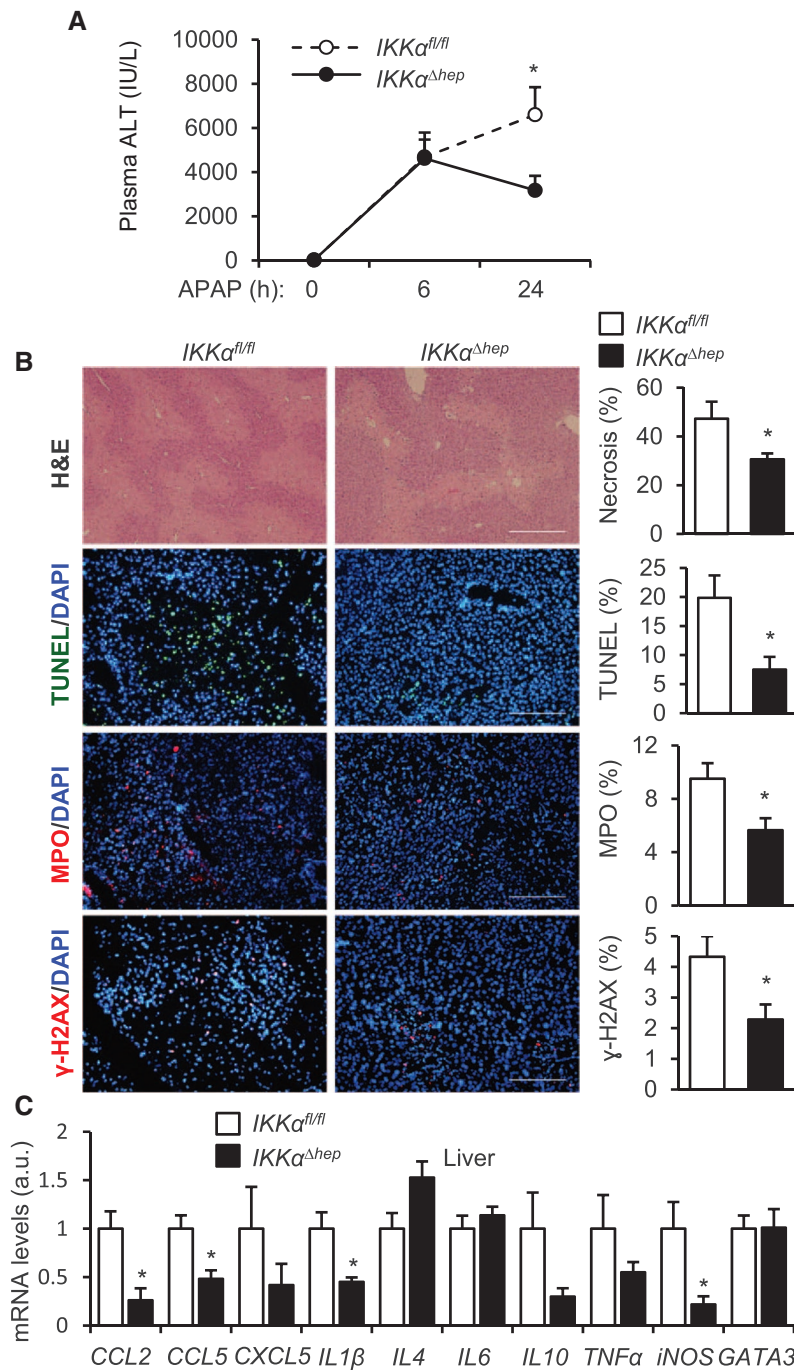


FIG. 4. *IKKα^{Δhep}* mice are resistant to APAP-induced liver damage. *IKKα^{Δhep}* and *IKKα^{fl/fl}* male mice were treated with APAP (250 mg/kg). (A) Plasma ALT levels. *IKKα^{Δhep}*, n = 9; *IKKα^{fl/fl}*, n = 10. (B) Liver sections were stained with the indicated agents (24 hours after APAP treatment, n = 3–8 per group). Scale bar, 200 μm. (C) Liver gene expression 24 hours after APAP treatment (normalized to 36B4 levels, n = 6–10 per group). Data are presented as mean ± SEM. **P* < 0.05; (B,C) two-tailed unpaired Student *t* test; (A) two-way ANOVA/Bonferroni's multiple comparisons test.

assess RNS, we stained liver sections with antibody to nitrotyrosine. Liver nitrotyrosine levels were significantly lower in *NIK^{Δhep}* (relative to *NIK^{fl/fl}*) and

IKKα^{Δhep} (relative to *IKKα^{fl/fl}*) mice, and were significantly higher in Hep^{NIK} than in Hep^{Con} mice (Fig. 5B). Considering that APAP induces oxidative stress

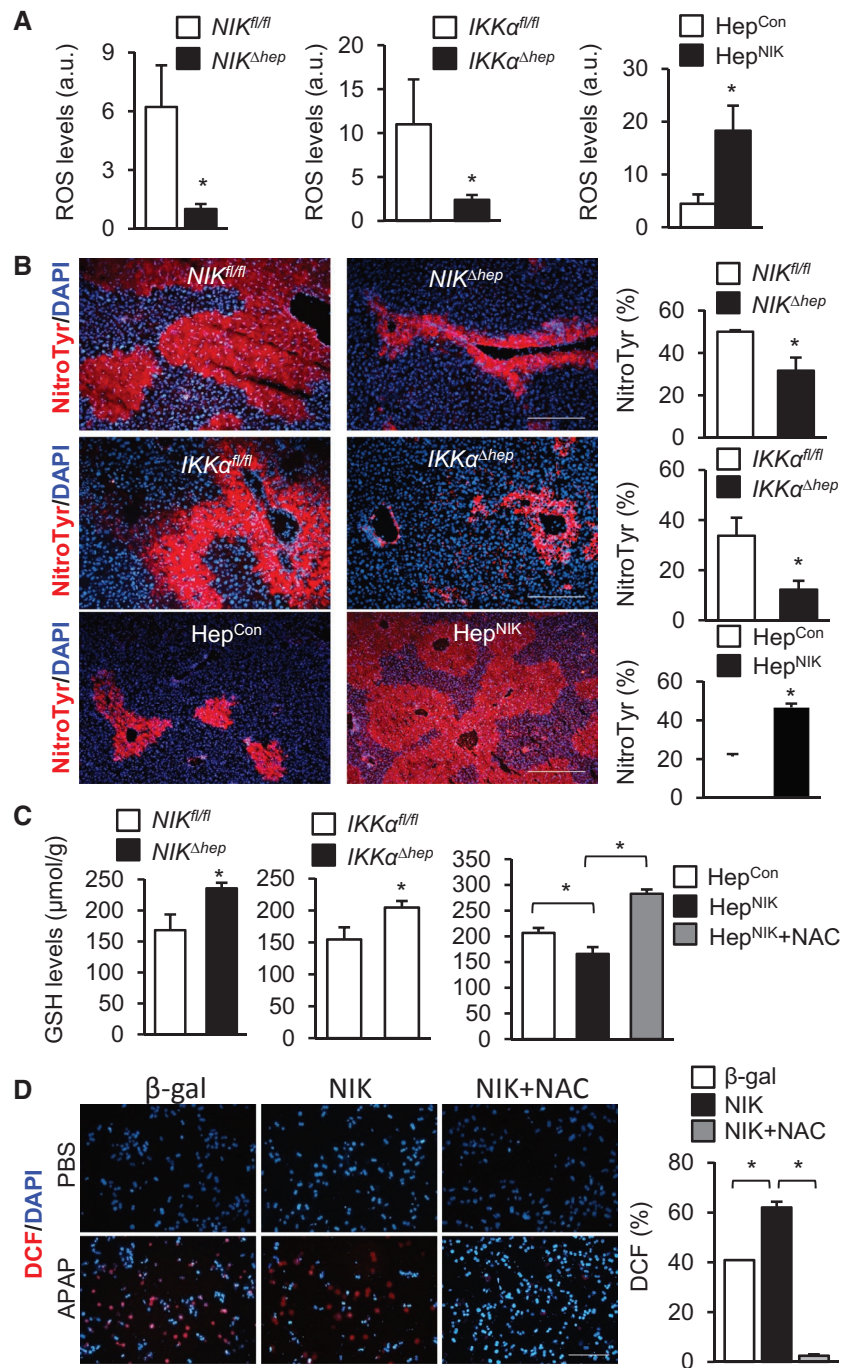


FIG. 5. NIK increases oxidative stress in hepatocytes. (A-C) Male mice were treated with APAP for 24 hours. Hep^{NIK} and Hep^{Con}, 200 mg/kg body weight; *NIK*^{Δhep}, *NIK*^{fl/fl}, *IKKα*^{Δhep}, and *IKKα*^{fl/fl}, 250 mg/kg. (A) Liver ROS levels (normalized to liver weight). *NIK*^{Δhep}, n = 7; *NIK*^{fl/fl}, n = 9; *IKKα*^{Δhep}, n = 6; *IKKα*^{fl/fl}, n = 9; Hep^{NIK}, n = 4; and Hep^{Con}, n = 4. (B) Liver sections were stained with anti-nitrotyrosine antibody. Nitrotyrosine area was normalized to total area. *NIK*^{Δhep}, n = 4; *NIK*^{fl/fl}, n = 4; *IKKα*^{Δhep}, n = 3; *IKKα*^{fl/fl}, n = 3; Hep^{NIK}, n = 4; and Hep^{Con}, n = 4. Scale bar, 200 μm. (C) Liver GSH levels (normalized to liver weight). *NIK*^{Δhep}, n = 10; *NIK*^{fl/fl}, n = 10; *IKKα*^{Δhep}, n = 9; *IKKα*^{fl/fl}, n = 7; Hep^{NIK}, n = 7; Hep^{Con}, n = 7; Hep^{NIK}+NAC, n = 4. (D) Mouse primary hepatocytes were transduced with NIK or β-gal adenoviral vectors, pretreated with 500 μM NAC, and followed by 2.5 mM APAP treatment for 24 hours. Hepatocytes were stained with DCF probes. DCF⁺ cells were normalized to total cells (n = 3 per group). Data are presented as mean ± SEM. **P* < 0.05 (A-C, left two panels) two-tailed unpaired Student *t* test. (C, right panel, D) two-way ANOVA/Bonferroni's multiple comparisons test. Abbreviation: NitroTyr, nitrotyrosine.

by depleting the glutathione (GSH) pool,⁽²⁾ we measured liver GSH levels. GSH levels were significantly higher in *NIK* ^{Δ hep} (relative to *NIK*^{fl/fl}) and *IKK α* ^{Δ hep} (relative to *IKK α* ^{fl/fl}) mice after APAP treatment (Fig. 5C). Conversely, liver GSH levels were significantly lower in Hep^{NIK} than in Hep^{Con} mice after APAP treatment, and treatment with the antioxidant NAC completely blocked GSH reduction (Fig. 5C).

To further validate the role of NIK in oxidative stress, we transduced mouse primary hepatocytes with NIK or β -gal adenoviral vectors, followed by APAP stimulation. Overexpression of NIK significantly increased ROS levels in APAP-treated hepatocytes, and NAC treatment completely blocked ROS elevations (Fig. 5D). Liver expression of inducible nitric oxide synthase (iNOS) was significantly lower in *NIK* ^{Δ hep} (relative to *NIK*^{fl/fl}) (Fig. 3D) and *IKK α* ^{Δ hep} (relative to *IKK α* ^{fl/fl}) mice (Fig. 4C). Conversely, liver iNOS expression was significantly higher in Hep^{NIK} than in Hep^{Con} mice (Fig. 2D). To verify that NIK directly increases iNOS expression in hepatocytes, we overexpressed NIK in mouse primary hepatocytes using NIK adenoviral vectors. NIK profoundly increased iNOS expression under both baseline and APAP-stimulated conditions (Supporting Fig. S4). These results show for the first time that the hepatic NIK/IKK α pathway augments liver oxidative stress in response to hepatotoxins, at least in part by increasing iNOS expression.

ROS IS INVOLVED IN NIK-INDUCED LIVER DAMAGE

To determine whether ROS mediates NIK action, we treated Hep^{NIK} mice with antioxidant NAC, followed by APAP stimulation. NAC dramatically decreased plasma ALT, liver ROS, and liver nitrotyrosine levels in APAP-treated mice (Fig. 6A-C). Importantly, NAC also drastically reduced liver necrosis (H&E), hepatocyte death (TUNEL), and liver neutrophil content (MPO) (Fig. 6C). Expression of CXCL5, IL1 β , TNF α , and iNOS in the liver was significantly lower in NAC-treated relative to empty vehicle-treated Hep^{NIK} mice (Fig. 6D). To corroborate these results, we transduced mouse primary hepatocytes with NIK or β -gal adenoviral vectors and treated hepatocytes with APAP in the presence or absence of NAC. Overexpression of NIK increased APAP-stimulated hepatocyte

death as expected, and NAC completely reversed NIK/APAP-induced hepatocyte death (Fig. 6E). Collectively, these results suggest that oxidative stress plays an important role in NIK-induced liver injury.

NIK ACTS CELL AUTONOMOUSLY TO PROMOTE HEPATOCYTE FERROPTOSIS

Given that ROS stimulates lipid peroxidation and ferroptosis, we speculated that NIK might augment hepatocyte ferroptosis. We transduced mouse primary hepatocytes with NIK or β -gal adenoviral vectors, followed by APAP stimulation. We blocked ferroptosis by treating hepatocytes with ferrostatin-1 or liproxstatin-1, two chemically distinct ferroptosis inhibitors. Overexpression of NIK markedly decreased the viability of APAP-treated hepatocytes, as assessed by MTT assays (Fig. 7A; β -gal vs. NIK). Treatment with either ferrostatin-1 or liproxstatin-1 markedly increased viabilities of both β -gal-expressing and NIK-expressing hepatocytes after APAP treatment (Fig. 7A). Liproxstatin-1 fully abrogated the ability of NIK to enhance APAP hepatotoxicity (Fig. 7A, right panels). Overexpression of NIK increased APAP-stimulated hepatocyte death (by TUNEL assays), and ferrostatin-1 or liproxstatin-1 profoundly inhibited hepatocyte death induced by NIK/APAP (Fig. 7B; Supporting Fig. S5).

To further validate ferroptosis, we examined the effects of NIK and APAP on production of lipid peroxides (ferroptosis marker), using the lipid peroxidation probe BODIPY 581/591 C11.⁽³²⁾ We transduced mouse primary hepatocytes with NIK or β -gal adenoviral vectors, stimulated cells with APAP, stained hepatocytes with BODIPY 581/591 C11, and assessed hepatocyte lipid peroxidation levels using flow cytometry. APAP increased BODIPY 581/591 C11 levels in β -gal adenoviral transduced hepatocytes (Fig. 7C,D). Overexpression of NIK considerably augmented the ability of APAP to increase BODIPY 581/591 C11 levels in hepatocytes (Fig. 7C,D). The frequency of C11^{high} hepatocytes was significantly higher in the NIK than in the β -gal groups after APAP stimulation (Fig. 7E). Using fluorescent microscopy, we confirmed that NIK overexpression augmented the ability of APAP to increase the C11^{high} hepatocyte number (Supporting Fig. S6).

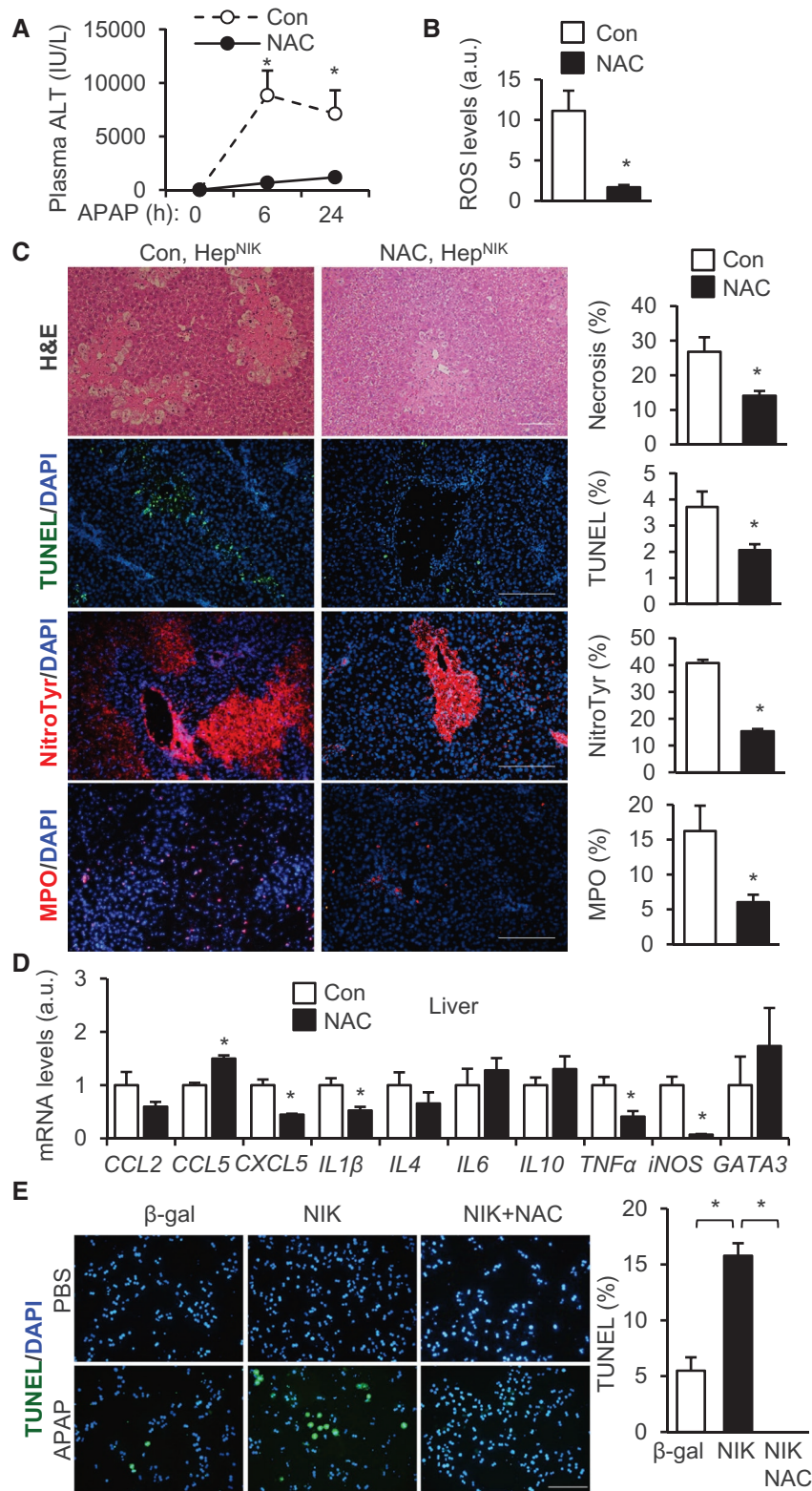


FIG. 6. Oxidative stress mediates NIK-induced liver injury. (A-D) Hep^{NIK} male mice were pretreated with NAC (300 mg/kg body weight) or empty vehicles (Con) and treated with APAP (200 mg/kg) for 24 hours. (A) Plasma ALT levels (n = 4 per group). (B) Liver ROS levels (normalized to liver weight, n = 4 per group). (C) Liver sections were stained with the indicated agents. Necrosis area, TUNEL⁺, MPO⁺, and nitrotyrosine cells were normalized to total area (n = 3-4 mice per group). Scale bar, 200 μ m. (D) Liver gene expression (normalized to 36B4 levels, n = 4 per group). (E) Mouse primary hepatocyte cultures were transduced with NIK or β -gal adenoviral vectors, pretreated with 500 μ M NAC, and followed by 2.5 mM APAP stimulation for 24 hours. Hepatocyte death was assessed by TUNEL assays (normalized to total cells, n = 3 per group). Data are presented as mean \pm SEM. **P* < 0.05; (B-D) two-tailed unpaired Student *t* test; (A,E) two-way ANOVA/Bonferroni's multiple comparisons test). Abbreviation: NitroTyr, nitrotyrosine.

We further validated ferroptosis using an antibody to 4-hydroxynonenal (4-HNE). We transduced mouse primary hepatocytes with NIK or β -gal adenoviral vectors, stimulated cells with APAP, and immunostained hepatocytes with an antibody to 4-HNE. APAP increased the number of 4-HNE⁺ hepatocytes; overexpression of NIK further increased 4-HNE⁺ hepatocytes (Fig. 7F). Treatment with antioxidant NAC abrogated the ability of NIK/APAP to increase 4-HNE⁺ hepatocytes (Fig. 7F). Taken together, these results unravel a previously unrecognized NIK/ROS/lipid peroxidation/ferroptosis axis.

Discussion

In this work, we have uncovered hepatic NIK and IKK α as previously unrecognized risk factors for acute liver failure. We observed that APAP, CCl₄, and possibly other hepatotoxins directly increase NIK expression and stability in hepatocytes. It is likely that these agents inhibit the abilities of tumor necrosis factor receptor-associated factor (TRAF)2, TRAF3, cellular inhibitor of apoptosis protein 1/2 (cIAP1/2), carboxy-terminus of Hsc70 interacting protein (CHIP), and/or related ubiquitin E3 ligases to promote the ubiquitination and degradation of NIK. Hepatocyte-specific overexpression of NIK substantially increased liver injury and mortality in mice treated with APAP. Hepatocyte death, DNA damage, and liver inflammation were markedly elevated in NIK-overexpressing mice after APAP treatment. Conversely, hepatocyte-specific ablation of NIK markedly decreased APAP-triggered acute liver failure and mortality. APAP-treated IKK α ^{*Δ*hep} mice phenocopied NIK^{*Δ*hep} mice. These findings reveal the hepatic NIK/IKK α pathway as an important player in drug-induced liver toxicity.

Liver-specific overexpression of NIK markedly increased liver ROS and RNS levels in APAP-treated

Hep^{NIK} mice. Conversely, ablation of either hepatic NIK or IKK α markedly decreased liver ROS and RNS levels in APAP-treated NIK^{*Δ*hep} or IKK α ^{*Δ*hep} mice, respectively. Liver GSH levels were also higher in NIK^{*Δ*hep} and IKK α ^{*Δ*hep} mice. These results indicate that endogenous hepatic NIK and IKK α are required for APAP and possibly other hepatotoxic drugs and agents to induce pathogenic oxidative stress in the liver. In line with this notion, in primary hepatocytes, overexpression of NIK increased ROS levels cell autonomously following APAP stimulation. Of note, overexpression of NIK increased whereas ablation of NIK decreased expression of iNOS in hepatocytes. iNOS deficiency mitigates alcoholic liver injury.⁽³³⁾ Hence, iNOS mediates, at least in part, NIK-promoted oxidative stress and liver injury.

Antioxidant NAC treatment reversed APAP/NIK-induced liver failure in Hep^{NIK} mice. NAC also blocked APAP/NIK-induced death in primary hepatocyte cultures. These results suggest that oxidative stress plays a pivotal role in NIK/APAP-induced liver failure. In line with this notion, DNA damage, presumably caused by ROS, was lower in NIK^{*Δ*hep} and IKK α ^{*Δ*hep} mice and higher in Hep^{NIK} mice relative to respective control mice after APAP treatment. DNA damage is likely to be involved in liver necrosis. ROS is well known to fuel lipid peroxidation. Accordingly, we found that overexpression of NIK increased the ability of APAP to stimulate production of lipid peroxides in hepatocytes (assessed by BODIPY 581/591 C11). 4-HNE levels were higher in NIK-overexpressing hepatocytes after APAP stimulation. Cell membrane lipid peroxidation in conjunction with iron overload is known to drive ferroptosis.^(11,12) Treatment with the chemically distinct ferroptosis inhibitors ferrostatin-1 and liproxstatin-1 blocked the ability of NIK/APAP to induce hepatocyte death. In accordance with these results, two groups recently reported that APAP induces ferroptosis in the liver.^(34,35) We acknowledge that some groups

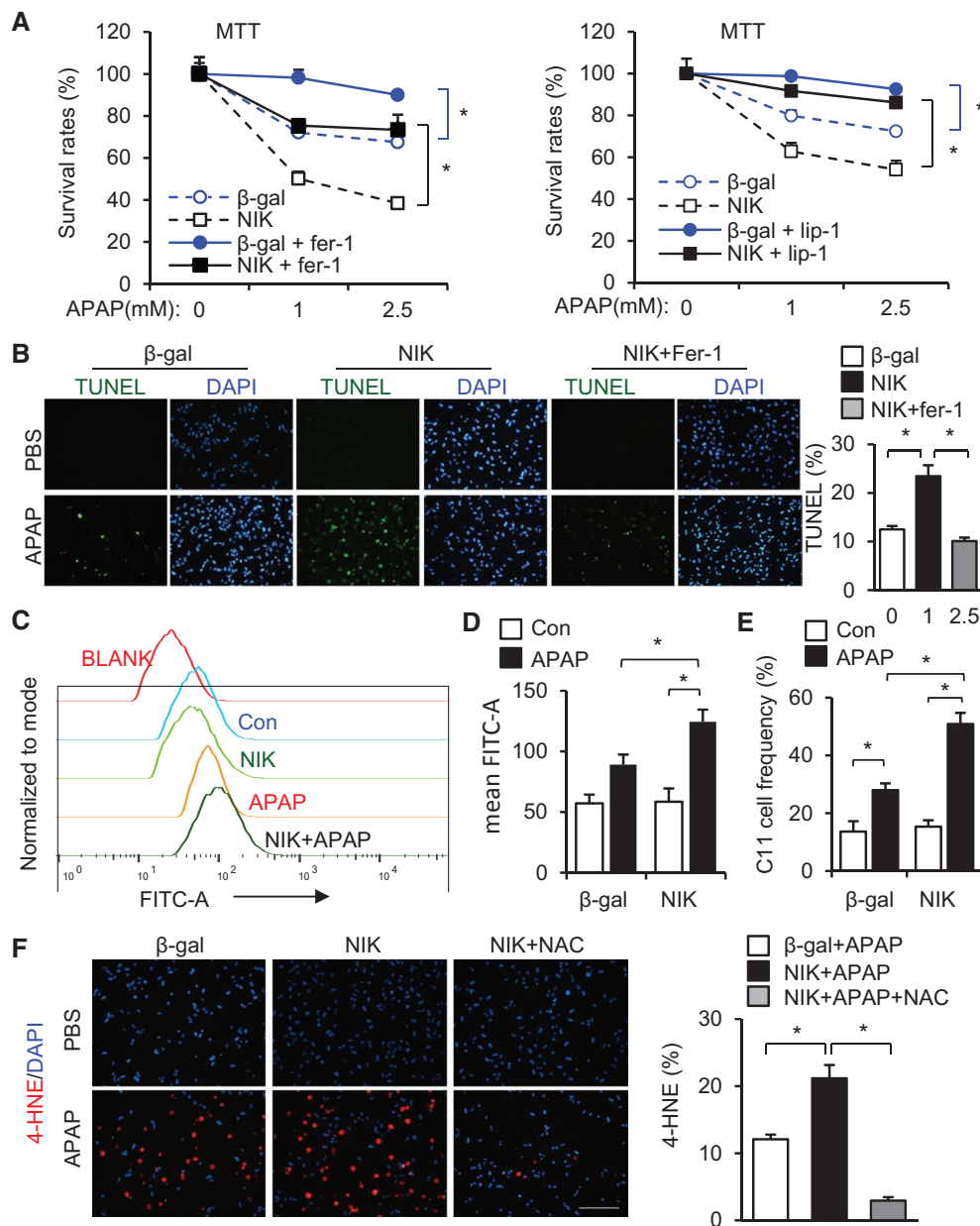


FIG. 7. NIK enhances ferroptosis of APAP-treated hepatocytes. (A,B) Mouse primary hepatocytes were transduced with NIK or β -gal adenoviral vectors, pretreated with 2 μ M ferrostatin-1 or 2 μ M liproxstatin-1, and followed by APAP stimulation for 24 hours. (A) MTT assays (n = 3 per group). (B) TUNEL assays (normalized to total cells, n = 3 per group). (C,D) Mouse primary hepatocytes were transduced with NIK or β -gal adenoviral vectors, treated with 2.5 mM APAP for 24 hours, stained with BODIPY 581/591 C11 probe, and analyzed by flow cytometry. (C) Representative C11 tracing. (D) Mean C11 density (n = 6 per group). (E) C11^{high} hepatocyte frequency (normalized to total hepatocytes, n = 6 per group). (F) Mouse primary hepatocytes were transduced with NIK or β -gal adenoviral vectors, treated with APAP for 24 hours in the presence or absence of 500 μ M NAC, and stained with anti-4-HNE antibody (normalized to total cells, n = 3 per group). Scale bar, 200 μ m. Data are presented as mean \pm SEM. **P* < 0.05; two-way ANOVA/Bonferroni's multiple comparisons test. Abbreviations: Fer-1, ferrostatin-1; Lip-1, liproxstatin-1.

consider ferroptosis not important for APAP hepatotoxicity.⁽³⁶⁾ We argue that the outcomes of APAP overdose are influenced by multiple genetic and non-genetic cofactors. Aberrant activation of the hepatic

NIK/IKK α /ROS/lipid peroxidation pathway likely augments hepatocyte ferroptosis. Of note, hepatic NIK modestly enhanced liver JNK activation in mice treated with APAP for 2 hours, raising the possibility

that JNK may be involved in mediating NIK/APAP-induced liver injury.

NIK has been extensively examined in lymph organ development and the immune system.⁽¹³⁾ Global *NIK* knockout results in thymus atrophy and autoimmune disorders (e.g., autoimmune hepatitis) in mice.⁽¹⁷⁾ Medullary thymic epithelial-specific deletion of *NIK* or *IKK α* impairs thymic medulla development and central T-cell tolerance, resulting in fatal autoimmune hepatitis in mice.⁽³⁷⁾ A modest elevation of hepatocyte *NIK* increases gluconeogenesis and suppresses fatty acid β oxidation in obesity, promoting metabolic disorders.^(16,20,22) Hepatic *NIK* and *IKK α* inhibit reparative hepatocyte proliferation by suppressing the JAK2/signal transducer and activator of transcription 3 pathway, impeding liver regeneration.⁽²³⁾ Excessive hepatic *NIK* promotes hepatocytes to release mediators that potently activate macrophages/Kupffer cells, and activated macrophages/Kupffer cells launch fatal immune destruction against the liver.⁽¹⁹⁾ Here, we found that hepatic *NIK* promotes liver oxidative stress and ferroptosis. Given that hepatic *NIK* is highly activated in a broad spectrum of liver injuries, we speculate that in both acute and chronic liver diseases, hepatic *NIK* serves as a common route connecting liver stress/inflammation to hepatocyte oxidative stress, ferroptosis, and liver injury. We further postulate that the pathogenic outcomes of hepatic *NIK* are influenced by *NIK* dosages and cofactors. Additional studies are warranted to delineate *NIK* dosage effects and identify cofactors regulating *NIK* responses.

Acknowledgment: We thank Dr. Klaus Rajewsky (Immune Disease Institute, Harvard Medical School, Boston, MA) for providing *Rosa26-STOP-NIK* mice; Dr. Lei Yin (University of Michigan) for providing Hepa1 cells; Dr. Cynthia Ju (University of Texas Health Science Center at Houston) for providing antibodies recognizing NAPQI adducts (originally from Dr. Lance R. Pohl, the National Heart, Lung, and Blood Institute, National Institutes of Health); Rashi Singhal, Xin Tong, and Lei Yin (University of Michigan) for helpful discussions; and Yankai Wen and Constance L. Atkins (University of Texas Health Science Center at Houston) for assistance in performing NAPQI adduct experiments.

REFERENCES

1) Rui L. Energy metabolism in the liver. *Compr Physiol* 2014;4:177-197.

- 2) Yan M, Huo Y, Yin S, Hu H. Mechanisms of acetaminophen-induced liver injury and its implications for therapeutic interventions. *Redox Biol* 2018;17:274-283.
- 3) Friedman SL. Mechanisms of hepatic fibrogenesis. *Gastroenterology* 2008;134:1655-1669.
- 4) Brenner C, Galluzzi L, Kepp O, Kroemer G. Decoding cell death signals in liver inflammation. *J Hepatol* 2013;59:583-594.
- 5) Bhattacharyya S, Sinha K, Sil PC. Cytochrome P450s: mechanisms and biological implications in drug metabolism and its interaction with oxidative stress. *Curr Drug Metab* 2014;15:719-742.
- 6) Masarone M, Rosato V, Dallio M, Gravina AG, Aglitti A, Loguercio C, et al. Role of oxidative stress in pathophysiology of nonalcoholic fatty liver disease. *Oxid Med Cell Longev* 2018;2018:9547613.
- 7) Louvet A, Mathurin P. Alcoholic liver disease: mechanisms of injury and targeted treatment. *Nat Rev Gastroenterol Hepatol* 2015;12:231-242.
- 8) Cichoż-Lach H, Michalak A. Oxidative stress as a crucial factor in liver diseases. *World J Gastroenterol* 2014;20:8082-8091.
- 9) Sohal RS. Role of oxidative stress and protein oxidation in the aging process. *Free Radic Biol Med* 2002;33:37-44.
- 10) Finkel T, Holbrook NJ. Oxidants, oxidative stress and the biology of ageing. *Nature* 2000;408:239-247.
- 11) Conrad M, Kagan VE, Bayir H, Pagnussat GC, Head B, Traber MG, et al. Regulation of lipid peroxidation and ferroptosis in diverse species. *Genes Dev* 2018;32:602-619.
- 12) Galaris D, Barbouti A, Pantopoulos K. Iron homeostasis and oxidative stress: an intimate relationship. *Biochim Biophys Acta Mol Cell Res* 2019;1866:118535.
- 13) Thu YM, Richmond A. NF-kappaB inducing kinase: a key regulator in the immune system and in cancer. *Cytokine Growth Factor Rev* 2010;21:213-226.
- 14) Xiao G, Harhaj EW, Sun SC. NF-kappaB-inducing kinase regulates the processing of NF-kappaB2 p100. *Mol Cell* 2001;7:401-409.
- 15) Sun SC. The noncanonical NF-kappaB pathway. *Immunol Rev* 2012;246:125-140.
- 16) Sheng L, Zhou Y, Chen Z, Ren D, Cho KW, Jiang L, et al. NF-kappaB-inducing kinase (NIK) promotes hyperglycemia and glucose intolerance in obesity by augmenting glucagon action. *Nat Med* 2012;18:943-949.
- 17) Shen H, Sheng L, Xiong Y, Kim YH, Jiang L, Chen Z, et al. Thymic NF-kappaB-inducing kinase (NIK) regulates CD4+ T cell-elicited liver injury and fibrosis in mice. *J Hepatol* 2017;67:100-109.
- 18) Ren X, Li X, Jia L, Chen D, Hou H, Rui L, et al. A small-molecule inhibitor of NF-kappaB-inducing kinase (NIK) protects liver from toxin-induced inflammation, oxidative stress, and injury. *FASEB J* 2017;31:711-718.
- 19) Shen H, Sheng L, Chen Z, Jiang L, Su H, Yin L, et al. Mouse hepatocyte overexpression of NF-kappaB-inducing kinase (NIK) triggers fatal macrophage-dependent liver injury and fibrosis. *Hepatology* 2014;60:2065-2076.
- 20) Liu Y, Sheng L, Xiong Y, Shen H, Liu Y, Rui L. Liver NF-kappaB-inducing kinase (NIK) promotes liver steatosis and glucose counterregulation in male mice with obesity. *Endocrinology* 2017;158:1207-1216.
- 21) Zhang WS, Pan A, Zhang X, Ying A, Ma G, Liu BL, et al. Inactivation of NF-kappaB2 (p52) restrains hepatic glucagon response via preserving PDE4B induction. *Nat Commun* 2019;10:4303.
- 22) Li Y, Chen M, Zhou Y, Tang C, Zhang W, Zhong Y, et al. NIK links inflammation to hepatic steatosis by suppressing PPARalpha in alcoholic liver disease. *Theranostics* 2020;10:3579-3593.

- 23) Xiong YI, Torsoni AS, Wu F, Shen H, Liu Y, Zhong X, et al. Hepatic NF- κ B-inducing kinase (NIK) suppresses mouse liver regeneration in acute and chronic liver diseases. *Elife* 2018;7:e34152.
- 24) Bernal W, Wendon J. Acute liver failure. *N Engl J Med* 2013;369:2525-2534.
- 25) Raucy JL, Lasker JM, Lieber CS, Black M. Acetaminophen activation by human liver cytochromes P450IIE1 and P450IA2. *Arch Biochem Biophys* 1989;271:270-283.
- 26) Kheradpezhoh E, Ma L, Morphett A, Barritt GJ, Rychkov GY. TRPM2 channels mediate acetaminophen-induced liver damage. *Proc Natl Acad Sci U S A* 2014;111:3176-3181.
- 27) Liu B, Xia X, Zhu F, Park E, Carbajal S, Kiguchi K, et al. IKK α is required to maintain skin homeostasis and prevent skin cancer. *Cancer Cell* 2008;14:212-225.
- 28) Zhou Y, Jiang L, Rui L. Identification of MUP1 as a regulator for glucose and lipid metabolism in mice. *J Biol Chem* 2009;284:11152-11159.
- 29) Jiang B, Shen H, Chen Z, Yin L, Zan L, Rui L. Carboxyl terminus of HSC70-interacting protein (CHIP) down-regulates NF- κ B-inducing kinase (NIK) and suppresses NIK-induced liver injury. *J Biol Chem* 2015;290:11704-11714.
- 30) Sasaki Y, Calado DP, Derudder E, Zhang B, Shimizu Y, Mackay F, et al. NIK overexpression amplifies, whereas ablation of its TRAF3-binding domain replaces BAFF:BAFF-R-mediated survival signals in B cells. *Proc Natl Acad Sci U S A* 2008;105:10883-10888.
- 31) Gao RY, Wang M, Liu Q, Feng D, Wen Y, Xia Y, et al. Hypoxia-inducible factor-2 α reprograms liver macrophages to protect against acute liver injury through the production of interleukin-6. *Hepatology* 2020;71:2105-2117.
- 32) Pap EH, Drummen GP, Winter VJ, Kooij TW, Rijken P, Wirtz KW, et al. Ratio-fluorescence microscopy of lipid oxidation in living cells using C11-BODIPY(581/591). *FEBS Lett* 1999;453:278-282.
- 33) McKim SE, Gäbele E, Isayama F, Lambert JC, Tucker LM, Wheeler MD, et al. Inducible nitric oxide synthase is required in alcohol-induced liver injury: studies with knockout mice. *Gastroenterology* 2003;125:1834-1844.
- 34) Wang M, Liu C-Y, Wang T, Yu H-M, Ouyang S-H, Wu Y-P, et al. (+)-Clausenamide protects against drug-induced liver injury by inhibiting hepatocyte ferroptosis. *Cell Death Dis* 2020;11:781.
- 35) Yamada N, Karasawa T, Kimura H, Watanabe S, Komada T, Kamata R, et al. Ferroptosis driven by radical oxidation of n-6 polyunsaturated fatty acids mediates acetaminophen-induced acute liver failure. *Cell Death Dis* 2020;11:144.
- 36) Jaeschke H, Adelusi OB, Ramachandran A. Ferroptosis and acetaminophen hepatotoxicity - are we going down another rabbit hole? *Gene Expr* 2021; <https://doi.org/10.3727/105221621X16104581979144>.
- 37) Shen H, Ji Y, Xiong Y, Kim H, Zhong X, Jin MG, et al. Medullary thymic epithelial NF- κ B-inducing kinase (NIK)/IKK α pathway shapes autoimmunity and liver and lung homeostasis in mice. *Proc Natl Acad Sci U S A* 2019;116:19090-19097.

Supporting Information

Additional Supporting Information may be found at onlinelibrary.wiley.com/doi/10.1002/hep4.1757/supinfo.